International Journal of
INTELLIGENT SYSTEMS AND APPLICATIONS IN ENGINEERING

ISSN:2147-6799 www.ijisae.org Original Research Paper

Fall Armyworm Detection on Maize Plants Using Gas Sensors, Image Classification, and Neural Network Based on IoT

D.Sheema[1] K.Ramesh[2] P.N.Renjith[3] Aiswarya.S[4]

Submitted: 13/08/2022 **Accepted:** 21/11/2022

***Abstract*:** Agriculture is pivotal to human health and for the growth of the nation, but to reap quality food, the maintenance of crops by evading pests is the vantage point. So, precision farming technology is very essential to solve this problem, and thereby it eases to yield more harvest. Crop health can be determined automatically from images which significantly paves the way to increase yields and profits for farmers along with reducing costs and time. In this study, two techniques have been proposed to solve the problem, (i) identifying the pest based on odor using gas sensors, and (ii) finding the pest infestation based on infected crops. Gas sensors are used as a substitute for human olfaction to detect gases emitting from pests. The FAW detection algorithm uses the Faster R-convolutional neural network (CNN) models VGG16, VGG19, MobileNetV2, and InceptionV3 to determine whether or not maize leaves have been infected. . Internet of Things (IoT) and Machine Learning are being used by the next generation of farmers to automate agricultural production and thereby eliminating the need for physical labour on the land while keeping on their crops. Models were developed to analyze pest and infected leaves which are captured by a Camera via remote sensing. Processes and actions are automatically triggered by the data and in specific environmental conditions to safeguard crops. Simulations were carried out using Shi-Thomas corner detection techniques. Compared to earlier proposed models, this proposed model is found to be relatively more accurate as well as more efficient. Also, the result for the object detection using odor increased to 8% compared with the previous detection and as a result of the modified image training, the models were found to be more accurate, having the accuracy range increasing from 93.35%, 93.32%, 98.01%, and 98.35% to 96.17%, 97.15%, 99.23%, and 99.13% respectively.

1. Introduction

In India, maize is cultivated throughout the year. India's third-largest cereal crop is maize followed by rice and wheat. As a major producer of maize, India ranks fourth in the field area and seventh in production, contributing around 4% of the world’s crop area and 2% of global production. Globally, 13% of malnourished children and 900 million poor households prefer corn as their staple food [1]. The maize crop has been plagued by various diseases and pests since 2016, and the most harmful pest was fall armyworms [2]. A study suggests that FAW may have been stowed away in cargo containers or aircraft holds of commercial planes before being dispersed by the wind throughout Africa. At least 12 African countries were infected by Faw, including Tanzania, from the western African tropics in 2016. In mid-May 2018, the occurrence of invasive fall armyworms on maize was reported for the first time in Karnataka, India [3]. Many studies have used digital cameras, unmanned aerial vehicles, and mobile phone cameras to photograph maize leaves remotely from farms to identify diseases and pests affecting them. Sensors and cameras were used in this study to capture images of the crop field to detect hidden pests. The Internet of Things allows devices on farms to measure a variety of data remotely, and share the information with the farmers in real-time. Devices connected to the Internet of Things can collect information like chemical application, soil moisture, dam levels, and livestock health. In addition, they can monitor fences, vehicles, and the weather. Farmers are forced to use a whole lot of chemicals on their crops to protect them from pests. It will be easier to ward off pests and eliminate pest infestation. Unfortunately, the repercussions of these also affect humans and animals by the changes.

The deep learning algorithm is used in this paper to resolve the issue. Objects and things can be located using the Internet of Things (IoT) and deep learning systems under any circumstance. In deep learning, object detection methodology is an efficient method of identifying objects accurately. This technology could potentially assist farmers in detecting pests at an early stage in order to prevent or mitigate damage. A primitive challenge for farmers is controlling pests at an early stage because it affects the growth and economy. The analysis of pests using odor substances has been developed in this study to improve productivity. Every pest exhibits different odors. Using odor detection, it is possible to locate hidden pests, like deep-buried or swirling in the leaves. So, the proposed system takes smells and odors as a key element, and uses five gas sensors to detect pungent, misty, sweet, and musty smells, followed with Faster R-CNN algorithm to extract features. Using an Odor-based object detection system, better accuracy can be attained and helps to avoid disseminating pest infestations. In this study, two patterns are used to analyze the objects: 1) Odor-based detection and 2) Corner classification with Feature Classification to determine whether the crops are infected. The two patterns are

[1,2,4]Hindustan Institute of Technology and Science, Tamilnadu, India.
[2]Sri Krishna College of Engineering and Technology, Tamilnadu, India.
[3] Vellore Institute of Technology, Tamilnadu, India.
sheemawilson20@gmail.com, rameshk.me@gmail.com, pn.renjith.it@gmail.com, aiswarya90@gmail.com

fully independent and perform separate tasks. The analysis is conducted via odor-based detection, which uses the foul smell of the pest to detect the pest. Due to some pests being small and camouflaged, this method is more accurate than previous methods for detecting them. Odors of pests are used to identify their chemical combinations, which allows to identify their species. Here, it was determined that the pest has an ammonia-like odor. The pest was also identified based on chemical combinations collected. The second pattern is feature classification based on corner detection, it can separate parameters and indicate whether an object has transpired or not, because previous methodologies only had predicted the object occurrences, so there was no confirmation whether the obstruction was a pest or not. hence, to classify the contaminants according to their shape, size, and color, an improved version of Faster R-CNN (I-SWFRN) was developed. Additionally, automated corner identification enhances the efficient identification of the affected area by identifying hidden objects. There are several models that can detect objects quickly and accurately, such as Faster R-CNN, Mask R-CNN, Fast R-CNN, Yolo, etc. Although faster R-CNNs perform better than others, their time-consuming nature will lead to inevitable consequences. With the improvement of Faster R-CNN, developed a new algorithm based on the processing and classification of images of captured leaves using improved convolutional neural networks (CNNs). InceptionV3, MobileNetV2, and VGG16 were used to determine whether leaves are affected by FAW. The accuracy of the models was improved to 93.35, 93.32%, 97.15%, 98.01%, and 99.23% using the Shi-Tomas corner detection technique for VGG16 and VGG19, as well as MobilenetV2 and InceptionV3.

The paper is divided into five sections: the second section reviews related research. The methodology of the study is discussed in Section 3. The findings and performance analysis are described in sections 4 and 5. Section 6 presents the conclusion.

2. Related Research

The background study found several publications dealing with odors and features. Wu.et.al developed a CNN model that could unveil pleasant and unpleasant smells more accurately than manual segmentation [5]. The model developed by Sharma, Anju, et.al envisage the correlation between chemical structure and smell by combining neural networks with image data [6]. As per Guo et al, LSTMs can be used to learn spatial and temporal features from E-nose signals to find smells through convolutional learning. [7]. Tengteng Wen, et.al developed a CNN encoder and decoder with odor-labeling for odor identification in machine olfaction and evaluated for effectiveness [8]. Lucy, et.al generate time-series data, test samples were attached to a pressure sensor, similar to a dog's sniff. By using this sensor, the smell can be identified and categorised [9]. According to Jana et.al, CNN was proposed as a way to detect rotten and fresh fruits respectively from the images [10]. In their study, Xiong et. using the computational efficiency of Spiking neural networks, and a convolutional Spiking neural network odor recognition algorithm was developed. [11]. Deep Learning has gained popularity because it can produce high-quality crop infestation identification in a very short period, and it can extract valuable information from large image datasets [12]. Bhatt et al. Adaptive boosting cascading, in conjunction with CNN-based decision tree classification, was used to segment corn leaf images into four categories: healthy, late blight, common rust, and leaf spot [13]. Ahila Priyadharshini et.al proposed a modified LeNet-based architecture for categorizing maize leaf infestations. These maize leaf images were tested using the village plants dataset. This Modified LeNet uses principal component analysis (PCA) whitening to reduce the correlation between features available in maize leaves. Based on a modified LeNet classification system, 97.89% of maize leaves were identified among the northern leaf blight, common rust, gray leaf spot, and healthy. [14]. Uddin et al. experimented to show the advantages of using feature extraction overusing the entire original dataset in terms of cost-effectiveness and improved classification performance. In terms of space and time complexity, MNF provides the highest classification accuracy, whereas FPCA provides the lowest [15]. Fan et al. proposed a genetic programming approach including new functions, new terminals, and a new program representation. Using the new approach, features can be extracted, constructed, and classified automatically and simultaneously [16]. Chen et.al proposed an alternative bottleneck for the improvement of feature extraction, called Multipath feature recalibration DenseNet. Additionally, multipath dense blocks were constructed using the SqueezeExcitation (SE) module to represent the interdependent relation between Dense Blocks [17]. Sheema et.al Implemented five sensors for analyzing five different scents, such as pungent, misty, sweet, musty, etc., then combined Faster R-CNN with the analysis. [18]. Ye et.al Shows a brief assessment of recent advances in feature extraction, modeling, and sensor drift compensation for E-Nose, this review sums up recent advances in this area. [19]. Kumar et.al provides an overview of the major feature extraction techniques. A comparison of different feature extraction methods for various parameters is presented using two benchmark spectral images [20].

3. Methodology

3.1. Area of study

Approximately three hectares of land were covered in this study at Coimbatore, Tamil Nadu (India). Field observations were conducted through the days 15 to 21 November 2021. Identifying fields with infected symptoms on maize leaves was done over a period of five days, followed by a period of two days of photographing these fields. The infected leaves are usually found with short holes, flesh frass, and semi-transparent patches. The infection rate was higher in maize fields at Coimbatore. Data collection was done on a three-month-old maize plant.

3.2. Detection based on Odor

Deep Learning techniques allow neural networks to accomplish sundry amazing tasks. Today, deep learning is performing a larger scale of tasks that humans can’t do. A sense of smell simulation based on an E-Nose or electronic nose is the next step in deep learning [21]. In India, this device is not affordable for the farmers, as a majority of them live in, an average and poor economy. A Conceptual pest tracking process was developed using odor functionality. A Faster R-CNN-based system is specifically designed to detect Fall Army Worms (FAW). The proposed name for this system is I-SWFRN, ie. Improved Speckle Warner based on Faster R-CNN. A maize crop can be eaten by this pest at any stage of growth and is easy to spread. In the past, pest control techniques included traps, poisonous foods, and pesticides, but these methods are harmful to human and animal life. This method must be monitored regularly to be countered. Infestations of pests can be eliminated when this technology is used properly. The pest could be identified with ease by applying ensemble learning to the odor analysis-based technique. Object detection is typically limited to detecting only visible objects, but not camouflaged ones. This technique helps even to locate the precise area of the camouflaged object in dense areas. An unpleasant smell is often released from the early stage of the FAW pest, which is pungent.

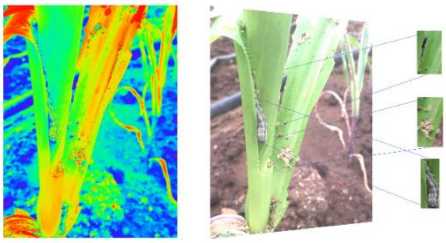

Figure 1: The detection of pests: a. Thermal Image b. Classification of features

Using this key technique, the pest can be identified even from a twirled leaf, and regular updates can be provided regardless of its location. This technique bonds the input of a chemical formula, which is obtained from Gas Sensors, and identifies the smell [22]. the pungent smell is primarily concentrated to identify the FAW and to find other species sweet smell, sting, minty, and pungent are used. Hence, the five odors of chemical combinations are taken in digital forms for analysis. As shown in Figure 1, pests can be detected. a. Pests are detected based on odor extracted from Thermal Camera features and b. Features are used to detect pests. In Figure 2. an infrared camera measures the values collected from five sensors. Using RGB images, the appearance, shape, and texture of each image will be displayed. Thermal cameras can capture images from a range of up to 60 degrees. The gas concentration is used to extract the features of compactness, speed, and long-term service from the sensor. Once the data has been retrieved from the storage, it can perform the prediction process. The below following formula is to determine the concentration of a chemical substance. According to Table 1, the pseudocode is applied to the concentration formula using the following characteristics.

$$f(gc) = \frac{gc_0 + gc_1}{gc_0} \qquad (1)$$

The concentration of odorous molecules f(gc) is represented by an odorous sample and an odorless sample. The odor units per cubic meter will be expressed as (ou/m^3).

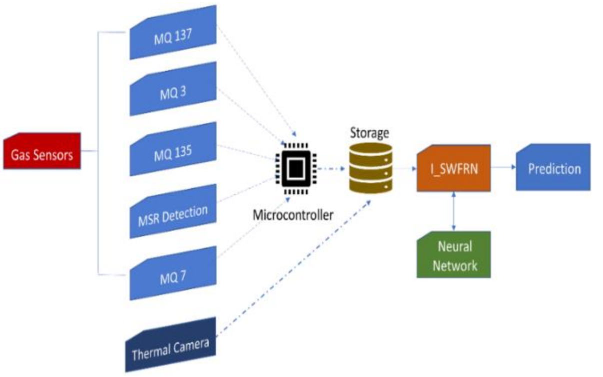

Figure 2: Process of Training data

```
Begin
            initialize gc into or
            set load gc into or
            read od from storage
              compare:
                    if gc>=400 ≈1   //ppm
            Then gc=$gc_0 + gc_1/gc_0$          --→ Applied
Equation (1)
   End
```

Table 1: Sensor for Odor Gases and the Sensitivity

Sensors	Sensitives	Chemical Name	Chemical Formula
MQ 3	Alcohol	Ethanol	C_2H_5OH
MQ 7	Sting	Formic Acid	HCOOH
MQ 135	Sweet smell	Methyl acetate	$C_3H_6O_2$
MQ 137	Pungent	Ammonia	NH3
MSR Detection	Minty	P-anisaldehyde	$C_8H_8O_2$

3.2.1 Thermal Camera

The infrared light of a thermal camera is used to measure temperature variations. An image sensor on a camera is made up of pixels that measure temperatures synchronously. The images are generated in RGB format and are displayed according to temperature format. There is no requirement for thermal cameras to be placed in dark environments, so they can work anywhere, regardless of how dark it is or how textured it is. Our work was conducted using a compact thermal camera called the SEEK thermal camera, which has 206 x 156 thermal sensors, a 36-degree field view, and measurements between 400 and 330 degrees Celsius. A thermal image with a frame rate of 9 Hz and 32,136 thermal pixels can be obtained [24]. The developed fusion model is trained and tested using gas sensors and thermal cameras simultaneously.

3.2.2 An Analysis of the Performance Matrix

The proposed model retrieves the gas sequence data by checking the similarity of the existing gas sequence and the retrieved data. An error message will be generated if a common object is not found, otherwise, the operation will continue as normal. An accurate classification was achieved using the four chemical properties of the pest described in Table 1. The accuracy, precision, recall, and F1 scores of Faster R-CNN and I-SWFRN are calculated in Table 2. A graphical representation of Faster R-CNN and I-SWFRN performance metrics can be found in Figures 3 and 4.

The following formula can be used to calculate the Average Precision, (Psà Precision Score, RsàRecall, FsàF1 Score)

$$Ps= \frac{T_{Pve+}\ T_{Nve}}{T_{Pve+}\ T_{Nve}\ +F_{Pve+}\ F_{Nve}} x100\% \quad \text{-------------------------(2)}$$

$$Rs= \frac{T_{Pve}}{T_{Pve+}\ T_{Nve}} x100\% \quad \text{------------}$$

-----------------------(3)

$$Fs= 2x\frac{Ps\ \ x\ \ Rs}{Ps\ \ +\ \ Rs} \quad \text{-------------------}$$

------------------------(4)

Table 2: A Performance Metric for Faster R-CNN using Odor Substance

Odor/Smell	No Gas	Pungent	Alcohol	Sting	Sweet Smell	Misty
Precision	0.99	0.86	0.85	0.84	0.83	0.89
Recall	0.99	0.89	0.87	0.89	0.85	0.91
F1 Score	0.99	0.87	0.88	0.9	0.85	0.88

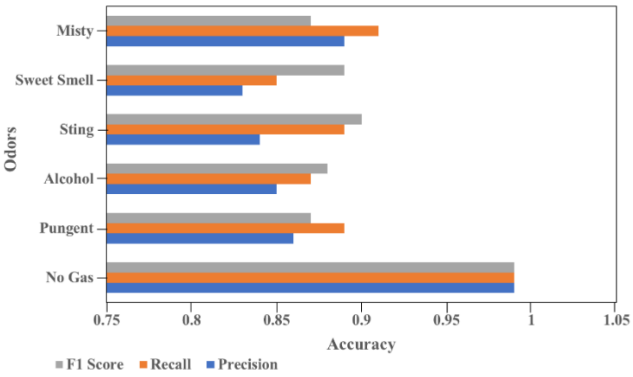

Figure 3: Performance Analysis of Faster R-CNN with Different Gases

Table 3: A Performance Metric for I-SWFRN using Odor Substance

Odor/Smell	No Gas	Pungent	Alcohol	Sting	Sweet Smell	Misty
Precision	1	0.94	0.91	0.89	0.91	0.9
Recall	1	0.93	0.9	0.9	0.92	0.91
F1 Score	1	0.93	0.9	0.9	0.92	0.91

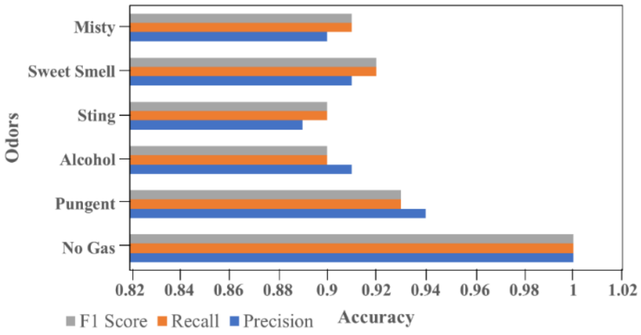

Figure 4: Performance Analysis of I-SWFRN with Different Gases

3.3 Feature Classification

The analysis of previous samples revealed that pests are impossible or harder to detect due to its tiny nature. In this sense, Faster R-CNN is not adequate for detecting the pest in maize fields on a large scale. With Faster R-CNN, convergence will take a long time since the anchors in RPN will come in 256 different sizes [25]. The Faster R-CNN model can identify the pest at any complexity level based on this intricate view. By combining multiple features, the I-SWFRN architecture can decrease computation time and improve operation speed. Further to separate overlapping boxes from single bounding boxes, non-max suppression is used. Images and other parameters, such as shape, size, and color, can be extracted more efficiently in this way. In Figure 6, the structure of the Improved-SWFRN network is shown.

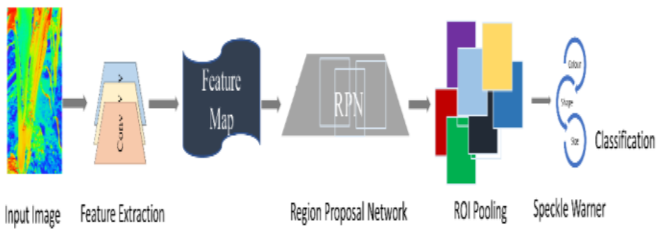

Figure 5: Proposed Architecture: Improved Speckle Warner based on Faster RCNN (I-SWFRN)

3.3.1 A method of detecting corners using Shi-Tomas

J.Shi and C. Tomasi (1994) proposed a technique to detect corners in images by examining significant variations in all directions. The Shi-Tomasi method is used by OpenCV to find the corners of the image to increase the effectiveness of the detection [26]. Based on Equation (2), pixels with an eigenvalue less than a threshold(R) are discarded, while the remaining pixels are sorted according to their quality ascendingly.

$$R = \min(\lambda 1, \lambda 2) \text{ -----> } (2)$$

In this case, R represents the predefined threshold and are eigenvalues of correlation. The below pseudocode is used to find the N-strongest corners in the image.

Pseudocode for Corner Detection

```
Begin
    Initialize img;
    Read img = imread (input);
    gy = implement convert operation
    // Corner_Det =cv2. goodFeaturesToTrack(gy,25,0.01,10)
   Corner_Det= np. into (Corner_Det)
   Set img into store(i) then
         i/nxn
Call loc (t,b,h,l)
Hl=1 then
Cal (size, shape,color)| no object found
    For i Σ c:
    Flatten parameter
    Circle(img,x,y)[3,255,-1]
    Output i;
End
```

3.3.2 Augmentation of Data

To augment the dataset for analysis, augmentation techniques can be used. Augmentation of data is the process of transforming existing data into current information without changing its form. Mirroring, rotating, shifting, and various photometric transformations are among the most commonly used augmentation techniques [27]. To increase the dataset, random rotations of 90^0 and flips of horizontal and vertical directions were applied. This helped to reduce overfitting in the training stage by extending the dataset. The augmented method with corner detection has been used in this study to increase the size of images to get better accuracy, as can be seen in Figure 6.

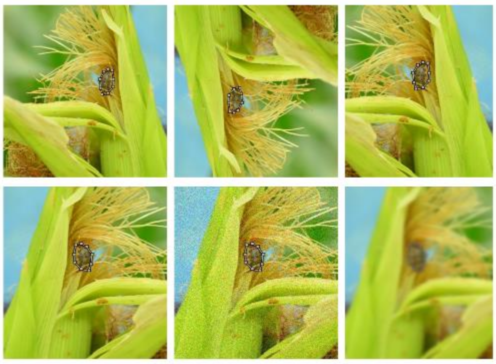

Figure 6: Data Augmentation with Corner Detection

3.3.3 Convolutional Neural Network

Recent years have seen a rise in the popularity of machine learning methods, especially neural networks. ANNs (artificial neural networks) are the primary type of neural network. A huge amount of training data is generated by connecting the neurons from prior layers. The three types of layers in CNN are convolution, pooling, and fully connected [27]. Layers such as convolution and pooling are used to map these extracted features into outputs.

According to our previous analysis, the pests FAW can hide inside plants and are tiny. Due to the small scale of this pest, Faster R-CNN cannot detect it in the maize field. In Faster R-CNN, 256 different anchor sizes are trained on a single image, so convergence is slow. This complex view of pests improves the accuracy of the Faster R-CNN model. By increasing the number of maps in the I-SWFRN architecture, feature fusion reduces computation time and speeds up the network. Non-max suppression is also used to determine the exact bounding box from the overlapped boxes. Hence, it is then possible to extract constraints like color, shape, and size from an image.

3.3.4 Transfer Learning

Several neural network training methods exist, including training from scratch and transfer learning. Before applying network weights to new tasks, transfer learning uses pre-trained network weights [28]. By applying network weights to generalize, better results can be achieved. In the study, CNN-based models (VGG16, VGG 19, Inception V3 and Mobilenet V2) were used and trained with the transfer learning technique to reduce cost and compute time. With 16 layers and 3*3 sized filters, the VGGNet consists of 16 convolutional layers. A neuron’s receptive field measures 5*5 when two 3 * # layers are stacked. A stacked 3 * 3 layer had 18 parameters, whereas a stacked 5 * 5 layer had 25, resulting in a reduction in parameters. Two convolutional layers can be attached instead of just one Rectified Linear Unit (ReLU) layer. There are only three convolution layers and two pooling layers in VGG16 and VGG19. As a result, the classifier has two layers with 4096 nodes each. Images taken as input by connected layers have a size of 224 * 224 pixels. Instead of using more layers, an inception module has been used which reduces the memory space and power consumption. The inception V3 model was developed as a successor to the InceptionV1 and InceptionV2 models. Consequently, the network’s parameters are reduced while fully connected layers are replaced with typical pooling at the top. The model identified 1000 classes on the ImageNet dataset with a top 5 error rate of 3.5% and a top 1 error rate as low as 17.3% from images with a 299 x 299-pixel size. Memory management is more efficient with this model than with other CNNs [29]. In addition, MobileNet is an embedded system model proposed by Google. The model builds thin deep neural networks by using depth-wise separable convolutions, compared to GoogleNet and Inception models. MobileNet is a lightweight framework developed by Google for embedded systems and mobile devices [30]. In this model, depth-wise separable convolutions are used to decrease the number of parameters required to train a network. The result is that it is easier to shape thin deep neural networks than Inception V3 and GoogleNet models.

3.4 The Results

The following section describes the experiment's setup, the parameters that defined the evaluation model, and the results. Images were taken using the Phantom 4 Pro v2 quadcopter drone, which has a built-in camera that has a resolution of 5472*3078 pixels and an aperture of F/2.8 at infinity. In total, 189 pictures were taken at 5m altitude on both fields. To maintain the same altitude during image capture, the drone was manually controlled. By using Python code (python 3.7 and pillow 6.0), the collected images were cropped into 450 x 300 pixels. OpenCV (open-source computer vision) was used to process and classify the images using the Shi-Tomasi corner detector method. Infected, non-infected, and background images were categorized from a 150 x 150 pixel cropped image. As the leaf was infected, it shows the indication of infestation, the non-infected group had images of healthy individuals and the background group consisted of grass, a tree trunk, and soil. The Figure illustrates the process used to acquire the images used in the experiments. Two groups of images were considered during training, ie infected and non-infected. These two groups contained a total of 11280 images, where 5670 are infected images and 5640 are non-infected images. The training set (7896), validation set (1692), and test set (1692) were divided by a ratio of 70:15:15. The models were developed using TensorFlow 2.0 and Python. Tensorflow's codes are easy to customize since they are written as low-level libraries, whereas Python has a large number of libraries and a moderate learning curve. With momentum of 0.9, a learning rate of 0.01, and a dropout rate of 0.2, stochastic gradient descent was employed to optimize the model. Based on these parameters, the optimizer produced a good result. The training was performed on a machine equipped with an Intel Core i5-7200u CPU running at 2.50 GHz and 2.71 GHz with 16 GB of memory. When it comes to image processing, the Shi-Tomas corner detector can be applied to the dataset to detect additional images. Both the original and modified images were subjected to a corner detection algorithm for model training. Model training takes a long time. This translates to a total of 5 hours for the MobileNetV2 model, 7 hours for the InceptionV3 model, 8.5 hours for the VGG16 model, and 9 hours for the VGG19 model. All four models were trained at the same time with modified and original images. Training VGGNet-based models take a long time because of the large number of parameters involved. A total of 30 training sessions were conducted on all four models to confirm the accuracy. Based on the training and validation sets, the models were evaluated and compared.

3.4.1 Metrics for Evaluation

Evaluation of the classification models was based on accuracy, specificity, sensitivity, precision, and F1-score. The accuracy of a sample statistic refers to how close it is to a parameter of the population. It is calculated by taking the sum of the correct predictions and dividing it by the total predictions. Equation (3) can be used to represent accuracy.

$$A = \frac{tn+tp}{tn+tp+fn+fp} \qquad ----\rightarrow 3$$

Incorrectly predicting true positives, true negatives, and falsely negative outcomes is possible in the model. The model predicts the positive class correctly if Tp (True Positive) is a true positive and the negative class correctly if Tn (True Negative).

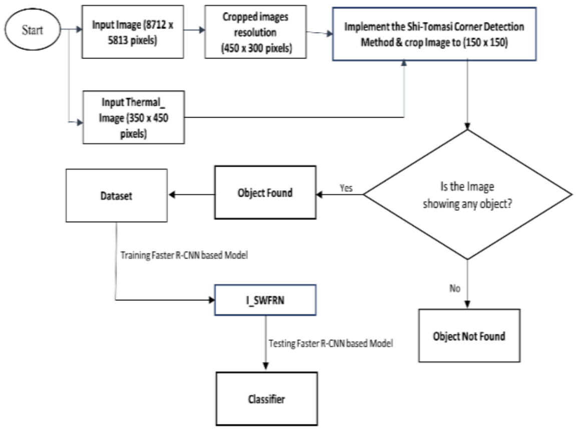
Start
Input Image (8712 x 5813 pixels)
Cropped images resolution (450 x 300 pixels)
Implement the Shi-Tomasi Corner Detection Method & crop Image to (150 x 150)
Input Thermal_ Image (350 x 450 pixels)
Dataset
Object Found
Yes
Is the Image showing any object?
Training Faster R-CNN based Model
I_SWFRN
No
Object Not Found
Testing Faster R-CNN based Model
Classifier

Figure 7: A Description of the methods used

Using the number of true positives divided by the number of false positives and false negatives, the sensitivity of the test can be determined. A dataset's relevance is determined by finding all relevant instances in it. Equation (4) depicts a dataset's sensitivity.

$$\text{Sensitivity (SE)} = \frac{tp}{tp+fn} -----\rightarrow 4$$

Based on Zhao et. al, specificity can be calculated by dividing true negatives by total negatives. Equation (5) represents specificity.

$$\text{Specificity (SP)} = \frac{tn}{tn+fp} --------\rightarrow 5$$

By dividing the number of true positives by the number of false positives, a precision ratio can be calculated.

$$\text{Precision (PN)} = \frac{tp}{tp+fp} --------\rightarrow 6$$

Additionally, F1 scores are needed when it comes to balancing precision with sensitivity. In comparison to the accuracy metric, it gives a more realistic picture of correctly classified cases.

$$\text{F1\_Score} = 2 * \frac{PN*SE}{PN+SE} --------\rightarrow 7$$

An infected image is classified as sensitive if it can be detected using a model, but as specific if it can be excluded from the classification. Precision values with a high level of accuracy will result in fewer false positives and therefore a better classification. furthermore, a higher F1-score value indicates the model classifier has performed well. Performance parameters are said to be better if they are close to 1, indicating that a model has reached its steady state.

3.4.2 Results of the experiment

The original images are used to train the models, as shown in figure 4. Based on fig 1, the VGG19-based model and the VGG16-based model are not significantly different in precision 4(a) and (b). The accuracy of the model based on VGG16 is 92.26%, while the accuracy of the model based on VGG19 is 92.32%. Further, the InceptionV3 model and MobileNetV2 model were not too different in precision, which is shown in Figures 4 (c) and (d). Model InceptionV3 was computed with a 96.75% accuracy, while model MobileNetV2 was computed with a 97.93% accuracy. The training curve was near to the validation curve in all four models. Validation curves are used to assess model performance. Fig 2 illustrates the accuracy of the trained model on revised images. In figure 3, the accuracy values for the original model, based on VGG16 and VGG19, were quite similar. It was found that the VGG16 model has an accuracy of 98.17%, while the VGG19 model has an accuracy of 99.00%. Furthermore, both the InceptionV3 and MobileNetV2 models were highly accurate, as shown in the following figures. According to InceptionV3 and MobilenetV2, both models were 100% accurate. In consequence, the modified images improved the performance of the models. From 92.26% to 98.17%, accuracy for a model based on VGG16 has increased, while that for a model based on VGG19 has increased from 92.32% to 99.00%. In addition, the MobileNetV2 model's accuracy increased from 97.93% to 99.00%, while the InceptionV3 model's accuracy increased from 96.75% to 99.00%. A few epochs of running the modes produced steady-state accuracy values, which means that the modes must have been run for a long time with revised images, but a short run was sufficient since Shi-Tomasi corner detection tracked both short holes and windowpanes. As a result, the classifier could generalize images quickly.

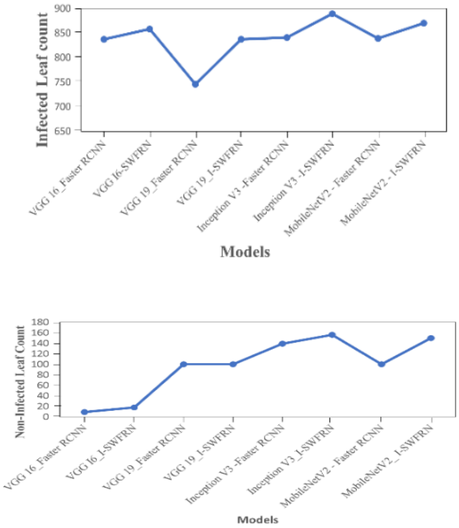

Figure 8: Comparison between Infected leaf and Non-Infected Count

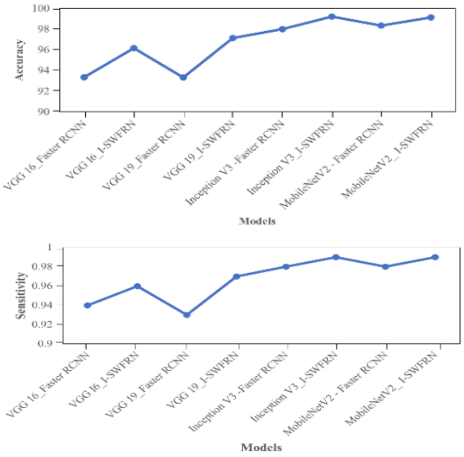

Figure 9: Accuracy Prediction

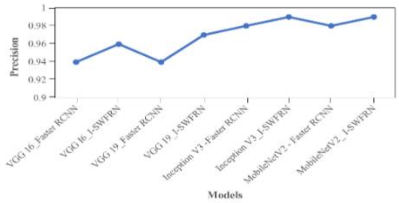

Figure 10: Sensitivity Prediction

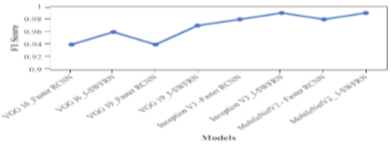

Figure 11: Precision Metrics

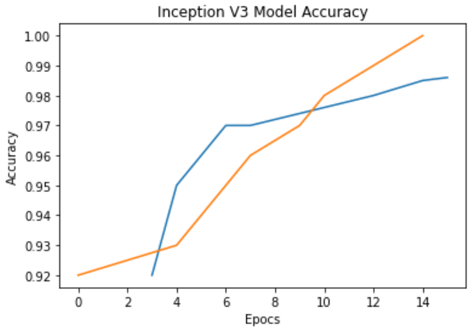

Figure 12: F1-Score Metrics

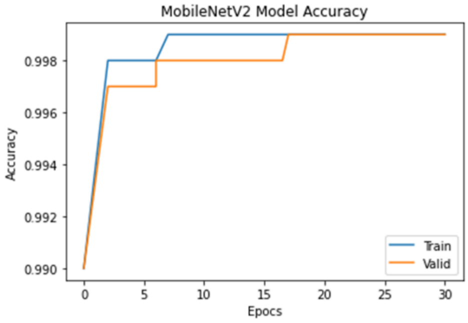

Figure 13: Working Process of I-SWFRN with InceptionV3 and MobileNetV2 models

The classification performance of the models is summarized in Table 3. Images modified with the labels VGG I6- I SWFRN, VGG 19_I-SWFRN, Inception V3 -I-SWFRN, and MobileNetV2 - I-SWFRN were used as input images, whereas original images were used with the labels VGG16_Faster RCNN, VGG19_Faster RCNN, InceptionV3_Faster RCNN, and MobileNetV2_Faster RCNN. The accuracy of the modified versions of VGG16, VGG19, InceptionV3, and MobileNetV2-mod is 96.17%, 97.15%, 99.23%, and 99.13%, respectively, as shown in Table 3. This is a substantial enhancement over the performance of the original models, which were VGG16 (93.33%), VGG19 (93.23%), InceptionV3 (9.91%), and MobileNetV2 (9.13).

Table 3: Classification Performance of the Models

Class	Infected	Not Infected	Accuracy	Sensitivity	Specificity	Precision	F1 Score
VGG 16_Faster RCNN	837	9	93.35	0.94	0.94	0.94	0.94
VGG I6-I-SWFRN	**858**	**18**	**96.17**	**0.96**	**0.96**	**0.96**	**0.96**
VGG 19_Faster RCNN	746	100	93.32	0.93	0.94	0.94	0.94
VGG 19_I-SWFRN	**837**	**100**	**97.15**	**0.97**	**0.97**	**0.97**	**0.97**
Inception V3 -Faster RCNN	841	139	98.01	0.98	0.98	0.98	0.98
Inception V3 -I-SWFRN	**889**	**156**	**99.23**	**0.99**	**0.99**	**0.99**	**0.99**
MobileNetV2 - Faster RCNN	839	100	99.10	0.98	0.98	0.98	0.98
MobileNetV2 - I-SWFRN	**870**	**150**	**99.13**	**0.99**	**0.99**	**0.99**	**0.99**

Relatively all the four models have been significantly improved in accuracy, but the InceptionV3-mod and MobileNetV2-mod networks achieved the highest accuracy of 99%. They achieve excellent performance with a minimal number of training cycles because they have a limited number of trainable parameters. According to Table 3, models with revised images perform better in terms of sensitivity, specificity, precision, and F1-score than models with original images with 0.99 each for InceptionV3 and MobileNetV2, 0.98 for VGG16, and 0.99 for VGG19. InceptionV3 and mobileNetV2 were evaluated after reaching a steady state. Accordingly, the infected images are detected and classified with the highest accuracy by using modified images.

4. Conclusion

Three deep convolutional neural network models were compared to classify maize images infected with the fall armyworm: VGG16, VGG19, MobileNetV2, and InceptionV3. To detect short holes and windowpanes in images of maize (450*300 pixels), a Shi-Tomas corner detection method was applied during pre-processing. With this approach, the maize images were effectively identified with high precision, specificity, sensitivity, and F1 score. According to Inception V3 and MobileNetV2, the accuracy, sensitivity, and F1 score were 99.13 %. InceptionV3 and MobileNetV2 had 99 % accuracy, 99 % specificity, 99 % precision, and 99 % F1 score. A few signs will be identified by the MobileNetV2 lite and InceptionV3 lite models on the maize images captured by the camera in real-time, to be shared with the remote stations. It will also be challenging to identify the exact location where infections have occurred in the field. Pesticides do not need to be applied to the entire field once they are identified, especially in the early stages of an infection. As a result, treating infected fields that show early signs of infection will take less time and cost

References

[1] Murdia, L. K., et al. "Maize utilization in India: an overview." American Journal of Food and Nutrition 4.6 (2016): 169-176.

[2] Midega, Charles AO, et al. "A climate-adapted push-pull system effectively controls fall armyworm, Spodoptera frugiperda (JE Smith), in maize in East Africa." Crop protection 105 (2018): 10-15. Kumar, Kasi Indra, Kanchhi Maya Waiba, and Mohinder Singh. "First report of natural infestation of Ovomermis sinensis (Nematoda: Mermithidae) parasitizing fall armyworm Spodoptera sp.(Lepidoptera: Noctuidae) in Himachal Pradesh, India." (2021).

[3] Li, Ming, et al. "Odor recognition with a spiking neural network for bioelectronic nose." Sensors 19.5 (2019): 993.

[4] Wu, Danli, et al. "POP-CNN: Predicting odor pleasantness with convolutional neural network." IEEE Sensors Journal 19.23 (2019): 11337-11345.

[5] Sharma, Anju, et al. "SMILES to smell: decoding the structure–odor relationship of chemical compounds using the deep neural network approach." Journal of Chemical Information and Modeling 61.2 (2021): 676-688.

[6] Mo, Zhuofeng, et al. "FPGA implementation for odor identification with depthwise separable convolutional neural network." Sensors 21.3 (2021): 832.

[7] Guo, Juan, et al. "ODRP: A Deep Learning Framework for Odor Descriptor Rating Prediction Using Electronic Nose." IEEE Sensors Journal 21.13 (2021): 15012-15021.

[8] Wen, Tengteng, et al. "An Odor Labeling Convolutional Encoder–Decoder for Odor Sensing in Machine Olfaction." Sensors 21.2 (2021): 388.

[9] Withington, Lucy, et al. "Artificial neural networks for classifying the time series sensor data generated by medical detection dogs." Expert Systems with Applications 184 (2021): 115564.

[10] Jana, Susovan, Ranjan Parekh, and Bijan Sarkar. "Detection of Rotten Fruits and Vegetables Using Deep Learning." Computer Vision and Machine Learning in Agriculture. Springer, Singapore, 2021. 31-49.

[11] Xiong, Yizhou, et al. "An odor recognition algorithm of electronic noses based on convolutional spiking neural network for spoiled food identification." Journal of The Electrochemical Society 168.7 (2021): 077519.

[12] Liu, Yang, et al. "A survey and performance evaluation of deep learning methods for small object detection." Expert Systems with Applications 172 (2021): 114602.

[13] Bhatt, Prakruti, et al. "Identification of Diseases in Corn Leaves using Convolutional Neural Networks and Boosting." ICPRAM. 2019.

[14] Ahila Priyadharshini, Ramar, et al. "Maize leaf disease classification using deep convolutional neural networks." Neural Computing and Applications 31.12 (2019): 8887-8895.

[15] Uddin, Md Palash, Md Al Mamun, and Md Ali Hossain. "PCA-based feature reduction for hyperspectral remote sensing image classification." IETE Technical Review 38.4 (2021): 377-396.

[16] Fan, Qinglan, et al. "Genetic programming for feature extraction and construction in image classification." Applied Soft Computing (2022): 108509.

[17] Chen, Bolin, et al. "Multipath feature recalibration DenseNet for image classification." International Journal of Machine Learning and Cybernetics 12.3 (2021): 651-660.

[18] Sheema, D., et al. "Detection of pest using Odor substance based on Deep Learning Algorithms." 2021 5th International Conference on Electrical, Electronics, Communication, Computer Technologies and Optimization Techniques (ICEECCOT). IEEE, 2021.

[19] Ye, Zhenyi, Yuan Liu, and Qiliang Li. "Recent Progress in Smart Electronic Nose Technologies Enabled with Machine Learning Methods." *Sensors* 21.22 (2021): 7620.

[20] Xiong, Yizhou, et al. "An odor recognition algorithm of electronic noses based on convolutional spiking neural network for spoiled food identification." Journal of The Electrochemical Society 168.7 (2021): 077519.

[21] Jing, Tao, Qing-Hao Meng, and Hiroshi Ishida. "Recent progress and trend of robot odor source localization." IEEJ Transactions on Electrical and Electronic Engineering 16.7 (2021): 938-953.

[22] Hirata, Yusuke, et al. "Biohybrid sensor for odor detection." Lab on a Chip 21.14 (2021): 2643-2657.

[23] Liu, Kewei, and Chao Zhang. "Volatile organic compounds gas sensor based on quartz crystal microbalance for fruit freshness detection: A review." Food Chemistry 334 (2021): 127615.

[24] Kumar, Brajesh, et al. "Feature extraction for hyperspectral image classification: A review." International Journal of Remote Sensing 41.16 (2020): 6248-6287.

[25] Wu, Xiongwei, Doyen Sahoo, and Steven CH Hoi. "Recent advances in deep learning for object detection." Neurocomputing 396 (2020): 39-64.

[26] Pal, Sankar K., et al. "Deep learning in multi-object detection and tracking: state of the art." Applied Intelligence 51.9 (2021): 6400-6429.

[27] Xiao, Bo, and Shih-Chung Kang. "Development of an image data set of construction machines for deep learning object detection." Journal of Computing in Civil Engineering 35.2 (2021): 05020005.

[28] Wu, Bizhi, et al. "Application of conventional UAV-based high-throughput object detection to the early diagnosis of pine wilt disease by deep learning." Forest Ecology and Management 486 (2021): 118986.

[29] Shivappriya, S. N., et al. "Cascade object detection and remote sensing object detection method based on trainable activation function." Remote Sensing 13.2 (2021): 200.

[30] Lu, Xiaocong, et al. "Attention and feature fusion SSD for remote sensing object detection." IEEE Transactions on Instrumentation and Measurement 70 (2021): 1-9.

[31] Cheng, Gong, et al. "Prototype-CNN for few-shot object detection in remote sensing images." IEEE Transactions on Geoscience and Remote Sensing 60 (2021): 1-10.

[32] Zhang, Ning, et al. "FPGA implementation for CNN-based optical remote sensing object detection." Electronics 10.3 (2021): 282.

[33] Xiong, Yizhou, et al. "An odor recognition algorithm of electronic noses based on convolutional spiking neural network for spoiled food identification." Journal of The Electrochemical Society 168.7 (2021): 077519.

[34] Jing, Tao, Qing-Hao Meng, and Hiroshi Ishida. "Recent progress and trend of robot odor source localization." IEEJ Transactions on Electrical and Electronic Engineering 16.7 (2021): 938-953.

[35] Hirata, Yusuke, et al. "Biohybrid sensor for odor detection." Lab on a Chip 21.14 (2021): 2643-2657.

[36] Liu, Kewei, and Chao Zhang. "Volatile organic compounds gas sensor based on quartz crystal microbalance for fruit freshness detection: A review." Food Chemistry 334 (2021): 127615.